The catalytic performance and characterization of a durable perovskite-type chloro-oxide $SrFeO_{3-\delta}Cl_{\sigma}$ catalyst selective for the oxidative dehydrogenation of ethane

H.X. Dai, C.F. Ng and C.T. Au *

Chemistry Department and Center for Surface Analysis and Research, Hong Kong Baptist University, Kowloon Tong, Hong Kong, China
E-mail: pctau@hkbu.edu.hk

Received 30 September 1998; accepted 28 December 1998

The catalytic performances and properties of $SrFeO_{3-0.190}$ and $SrFeO_{3-0.382}Cl_{0.443}$ catalysts have been investigated for the oxidative dehydrogenation of ethane (ODE). XRD results showed that both catalysts exhibited oxygen-deficient perovskite-type structures. The inclusion of chloride ions in the $SrFeO_{3-\delta}$ lattice matrix can significantly enhance ethene selectivity and ethane conversion. The $SrFeO_{3-0.382}Cl_{0.443}$ catalyst showed an ethane conversion of ca. 90%, an ethene selectivity of ca. 70%, and an ethene yield of ca. 63% under the reaction conditions: $C_2H_6:O_2:N_2 = 2:1:3.7$, temperature 680 °C, and space velocity 6000 $ml\,h^{-1}\,g^{-1}$. With the increase of space velocity, ethane conversion decreased, whereas ethene selectivity increased over $SrFeO_{3-0.382}Cl_{0.443}$. Lifetime studies showed that the perovskite-type chloro-oxide catalyst was durable. The results of O_2-TPD and TPR experiments illustrated that the implanted chloride ions caused the oxygen nature of $SrFeO_{3-\delta}$ to change. By regulating the concentration of oxygen vacancies and the Fe^{4+}/Fe ratio in this perovskite-type chloro-oxide catalyst, one can generate a durable chloro-oxide catalyst for the ODE reaction with excellent performance.

Keywords: perovskites, $SrFeO_{3-\delta}Cl_{\sigma}$, chloro-oxides, selective oxidation, oxidative dehydrogenation, ferrates-based catalysts, ethane, ethene

1. Introduction

In the past decade, many efforts have been paid for the development of new catalysts for the oxidative dehydrogenation of ethane (ODE) to ethene. Generally speaking, the effective catalysts for the OCM (oxidative coupling of methane) reaction might be fit for the ODE reaction. Besides the alkaline earth, rare earth, and transition metal oxides with or without the use of alkali or halides as dopants (e.g., Li/MgO [1,2], Na/CeO_2 [3], SmOF [4], M–Mo or V/SiO_2 (M = Li, Na, K, Rb, and Cs) [5,6], M-ZSM-5 (M = Nb, V, Co, and Cu) [7]), the perovskite-type mixed oxides have also been reported to be effective in the OCM and ODE reactions. $LaCoO_{3-\delta}$-based mixed oxides [8], $SrCo_{0.8}Li_{0.2}O_3$ [9], $La_{0.8}Sr_{0.2}CoO_3$ and $SrCo_{0.8}Fe_{0.2}O_3$ [10], $CaCo_{0.8}Fe_{0.2}O_3$ [11], and $La_{0.6}Sr_{0.4}Co_{0.8}Fe_{0.2}O_3$ [12] exhibited moderate catalytic performance for the OCM reaction. Hayakawa et al. [13] studied the catalytic activities of $CaTi_{1-x}Fe_xO_{3-\delta}$ ($0 \leqslant x \leqslant 0.4$) and $SrTi_{1-x}Fe_xO_{3-\delta}$ ($0 \leqslant x \leqslant 1.0$) for the ODE reaction, and found that the latter showed higher C_2H_4 selectivity than the former. Recently, they reported the catalytic performance of $La_{1-x}Sr_xFeO_{3-\delta}$ ($0 \leqslant x \leqslant 1.0$) [14]. Under the reaction conditions of 650 °C, C_2H_6/O_2 molar ratio of 1/1, space velocity of ca. 7000 $ml\,h^{-1}\,g^{-1}$, a C_2H_6 conversion of 87% and a C_2H_4 selectivity of 43% with the corresponding C_2H_4 yield of 37% were obtained over a $SrFeO_{3-\delta}$ catalyst.

In the past several years, we have characterized and reported the La–Ba–X [15–18], Y–Ba–X [19,20], and Ho–Ba–X [21] catalysts for the OCM reaction and the Ho–Ba–X (X = F, Cl, and Br) [22,23] catalysts for the ODE reaction. We detected the occurrence of ionic exchange/substitution between Ba^{2+} and Ln^{3+} (Ln = La, Y and Ho) and/or X^- and O^{2-} ions in these BaX_2-modified rare earth oxide catalysts. Lattice defects generated in these catalysts, such as trapped electrons and charge-deficient oxygen, are able to facilitate the activation of gaseous oxygen molecules, a critical step for the conversion of ethane to ethene. We have also reported that the presence of halide ions in these catalysts could suppress the deep oxidation of ethane and ethene.

Perovskite-type mixed oxides have been studied intensively and extensively. These materials exhibit good catalytic performances in the complete oxidation of hydrocarbons [24], carbon monoxide [25] and ammonia [26]. We envisage that, by embedding halide ions in the lattice of perovskite-type mixed oxides, one may convert these deep oxidation materials to selective catalysts for the ODE reaction. By so doing, one might (i) suppress the deep oxidation of C_2H_6 and C_2H_4 (thus increasing C_2H_4 selectivity) and (ii) minimize the leaching of halide (thus prolonging the lifetime of catalysts). In this study, we present the catalytic performances and characterization of perovskite-type

---

* To whom correspondence should be addressed.

chloro-oxide $SrFeO_{3-\delta}Cl_\sigma$ as well as $SrFeO_{3-\delta}$ (for comparison purposes) for the ODE reaction. The investigation of $La_{1-x}Sr_xFeO_{3-\delta}X_\sigma$ (X = F, Cl; $x = 0$–1) will be reported elsewhere.

2. Experimental

The catalysts were prepared by adopting the method of citric acid complexing [27]. $SrCl_2{\cdot}6H_2O$ (Merck, >99%) and $Fe(NO_3)_3{\cdot}6H_2O$ (Acros, ⩾99%) (for $SrFeO_{3-\delta}Cl_\sigma$) or $Sr(NO_3)_2$ (Fluka, >99%) and $Fe(NO_3)_3{\cdot}9H_2O$ (Acros, ⩾99%) (for $SrFeO_{3-\delta}$) were mixed in aqueous solution at the desired stoichiometric ratio. Citric acid (monohydrate, Aldrich, 99.0%) equimolar to the metals was added. The solution was then evaporated at 70 °C to produce a viscous syrup. After subsequent evaporation at 100 °C for 5 h and calcination at 900 °C for 10 h, the material was in turn ground, pressed, crushed, and sieved to the size range of 40–80 mesh.

The ODE reactions were carried out at atmospheric pressure with 0.5 g of the catalyst being placed in a fixed-bed quartz micro-reactor (i.d. = 4 mm). The reaction temperatures were ranging from 420 to 680 °C at 20 °C intervals. A mixture of ethane and air was passed through the micro-reactor. The flow rate was regulated by a mass flow controller. It was 14.8 $ml\,min^{-1}$ for ethane and 35.2 $ml\,min^{-1}$ for air; giving a space velocity of 6000 $ml\,h^{-1}\,g^{-1}$ and a C_2H_6/O_2 molar ratio of 2/1. The product (C_2H_6, C_2H_4, CH_4, CO, and CO_2) distribution was determined on line by a gas chromatograph (Shimadzu 8A TCD) with Porapak Q and 5A Molecular Sieve columns. For the variation of space velocity, the catalyst mass was varied at a fixed flow rate of 50 $ml\,min^{-1}$.

The phase compositions of the catalysts were determined by X-ray diffraction (XRD, D-MAX, Rigaku). The specific surface areas of the catalysts were measured and calculated according to the BET method.

For the O_2-TPD (temperature-programmed desorption) studies, the samples (0.5 g) were placed in the middle of a quartz micro-reactor with 4 mm inner diameter. The outlet gases were analyzed on line by mass spectrometry (HP G1800A). The heating rate was 10 °C min^{-1} and the temperature range was from room temperature to 850 °C. Before performing the O_2-TPD experiments, the samples were first evaculated *in situ* at 850 °C for 1 h and then calcined at the same temperature for 1 h under an oxygen flow of 20 $ml\,min^{-1}$ followed by cooling in oxygen to room temperature and helium purging (flow rate, 20 $ml\,min^{-1}$) for 1 h.

Temperature-programmed reduction (TPR) was conducted by using a 7% H_2–93% N_2 (v/v) mixture. The flow rate of the carrier gas was 50 $ml\,min^{-1}$ and a thermal conductivity detector was used. The amount of sample used was 0.2 g and the heating rate was 10 °C min^{-1}. Before performing the TPR experiments, the sample was first calcined *in situ* at 850 °C for 1 h under an oxygen flow of 15 $ml\,min^{-1}$ followed by cooling in oxygen to room temperature.

For the analysis of Cl content, the catalyst was first digested in 0.1 M NaOH solution. The resulted solution was neutralized by 2 M HNO_3 solution and titrated against standardized $AgNO_3$ solution using 0.005 M potassium chromate as an indicator. The content of Fe^{3+} was determined by titrating the digested sample against $K_2Cr_2O_7$ in HCl (3 M) with an excess amount of Mohr salt [26]. The experimental error is estimated to be ±1.0%.

3. Results

3.1. Catalyst composition

Table 1 shows the compositions of $SrFeO_{3-\delta}$ and $SrFeO_{3-\delta}Cl_\sigma$. Based on the Fe^{4+}/Fe ratio and Cl content as well as the assumption of maintaining electrical neutrality, the value of δ is estimated to be 0.190 for $SrFeO_{3-\delta}$, whereas the values of δ and σ are, respectively, 0.382 and 0.443 for $SrFeO_{3-\delta}Cl_\sigma$. From table 1, one can also realize that the addition of chloride ions to $SrFeO_{3-\delta}$ has caused the Fe^{4+}/Fe ratio to rise and the oxygen vacancies to decrease in density.

3.2. Catalytic performance

Figure 1 shows the catalytic performances of $SrFeO_{3-0.190}$ and $SrFeO_{3-0.382}Cl_{0.443}$ after 1 h of on-stream ODE reaction. From figure 1(a), one can observe that, with the increase of reaction temperature from 500 to 680 °C, the C_2H_6 conversion, C_2H_4 selectivity, C_2H_4 yield, and CH_4 selectivity over $SrFeO_{3-\delta}$ increased from 33.7, 38.0, 12.8, and 0.3% to 54.8, 50.5, 27.7, and 2.3%, respectively, whereas CO_x (i.e., CO + CO_2) selectivity decreased from 61.7 to 47.2%. Over the $SrFeO_{3-0.382}Cl_{0.443}$ catalyst (figure 1(b)), when the temperature was raised from 420 to 540 °C, C_2H_6 conversion, C_2H_4 selectivity, and C_2H_4 yield increased, respectively, from 4.1, 29.2, and 1.2% to 52.1, 69.6, and 36.3%; between 540 and 600 °C, such increases were not significant. Further rise in temperature from 600 to 680 °C would cause the C_2H_6 conversion and C_2H_4 yield to rise rapidly from 57.9 and 41.1% to 89.9 and 62.2%, respectively, whereas C_2H_4 selectivity reached a maximum value of 73.6% at 640 °C and then decreased slightly. The CO_x selectivity dropped rapidly from 420 to 540 °C, but such drop was moderate at temperatures above 540 °C. We observed that CH_4 was generated gradually from 460 °C and between 620 and 680 °C, CH_4 selectivity increased from

Table 1
Compositions of $SrFeO_{3-\delta}$ and $SrFeO_{3-\delta}Cl_\sigma$ catalysts.

Catalyst	Fe^{4+}/Fe (%)	Cl content (%)	δ	σ
$SrFeO_{3-\delta}$	62.1	–	0.190	–
$SrFeO_{3-\delta}Cl_\sigma$	68.0	7.81	0.382	0.443

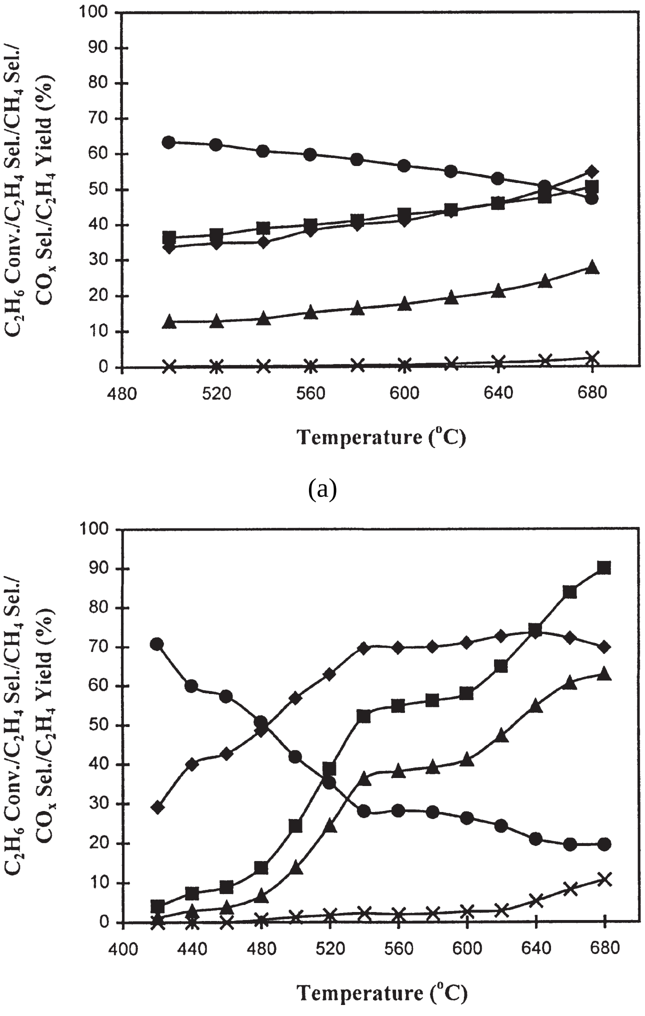

(a)

(b)

Figure 1. Catalytic performance of (a) $SrFeO_{3-0.190}$ and (b) $SrFeO_{3-0.382}Cl_{0.443}$ after 1 h of on-stream ODE reaction. (■) C_2H_6 conversion, (◆) C_2H_4 selectivity, (▲) C_2H_4 yield, (×) CH_4 selectivity, (●) CO_x selectivity.

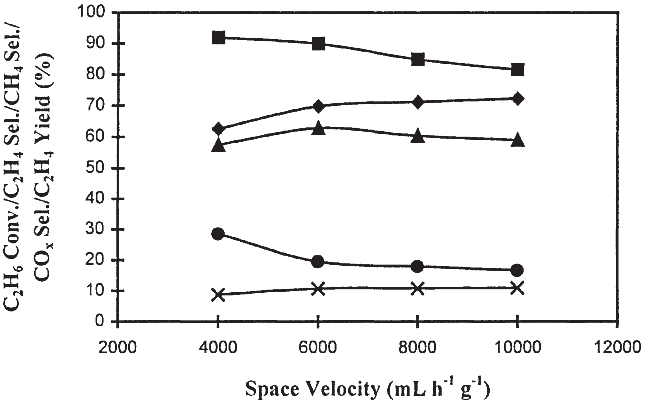

Figure 2. Catalytic performance of $SrFeO_{3-0.382}Cl_{0.443}$ as related to space velocity at 680 °C for the ODE reaction. (■) C_2H_6 conversion, (◆) C_2H_4 selectivity, (▲) C_2H_4 yield, (×) CH_4 selectivity, (●) CO_x selectivity.

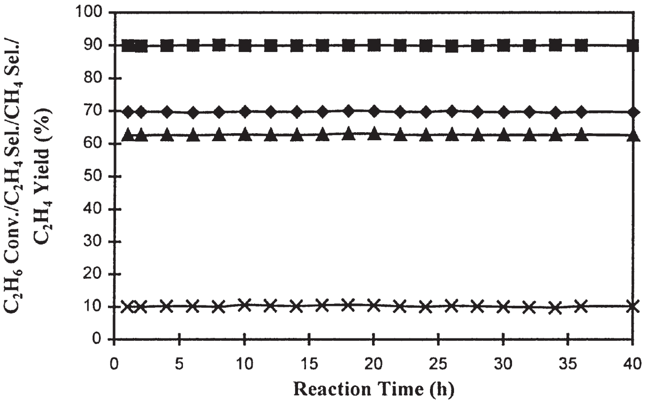

Figure 3. Life study of $SrFeO_{3-0.382}Cl_{0.443}$ at 680 °C during 40 h of on-stream ODE reaction. (■) C_2H_6 conversion, (◆) C_2H_4 selectivity, (▲) C_2H_4 yield, (×) CH_4 selectivity.

3.0 to 10.7%. It should be noted that the O_2 conversions were 100% during the studies.

Figure 2 shows the catalytic performance of $SrFeO_{3-0.382}Cl_{0.443}$ as a function of space velocity at 680 °C for the ODE reaction. With the increase of space velocity from 4,000 to 10,000 $ml\,h^{-1}\,g^{-1}$, C_2H_4 selectivity and CH_4 selectivity increased from 62.6 and 8.8% to 72.3 and 11.0%, respectively, whereas C_2H_6 conversion and CO_x selectivity decreased from 91.9 and 28.6% to 81.6 and 16.7%, respectively. The C_2H_4 yield reached a maximum value of 62.8% at a space velocity of 6,000 $ml\,h^{-1}\,g^{-1}$.

Figure 3 shows the catalytic performance of $SrFeO_{3-0.382}Cl_{0.443}$ as related to reaction time. Clearly, this catalyst showed stable performance during the 40 h of on-stream reaction. Such sustainable behaviour demonstrates the stability of the $SrFeO_{3-0.382}Cl_{0.443}$ catalyst during the reaction. The results of chemical analysis showed that the Cl contents of this catalyst before and after the reaction of 40 h were 7.81 and 7.79 wt%, respectively, indicating that there was no significant Cl loss during the 40 h period.

3.3. Phase composition and surface area

Figure 4 shows the XRD patterns of $SrFeO_{3-0.190}$ and $SrFeO_{3-0.382}Cl_{0.443}$ catalysts. Compared to the JCPDS 34-638 data, both $SrFeO_{3-\delta}$ and $SrFeO_{3-0.382}Cl_{0.443}$ had cubic perovskite structures [26,28]. Actually, a brownmillerite-like structure $ABO_{2.5}$ (such as $SrFeO_{2.5}$ [14] and $SrCoO_{2.5}$ [29]) could also be considered as an oxygen-deficient perovskite-type ABO_3 structure [26]. From figure 4, one can see that the patterns of a $SrFeO_{3-0.382}Cl_{0.443}$ catalyst before and after 40 h of on-stream ODE reaction are rather similar, indicating that there was no phase change during the 40 h of reaction. In other words, there was no significant Cl leaching. The stable performance of the $SrFeO_{3-0.382}Cl_{0.443}$ catalyst also confirmed such a conclusion. According to the BET method, the surface areas of $SrFeO_{3-0.190}$ and $SrFeO_{3-0.382}Cl_{0.443}$ were estimated to be 3.3 and 3.1 $m^2\,g^{-1}$, respectively.

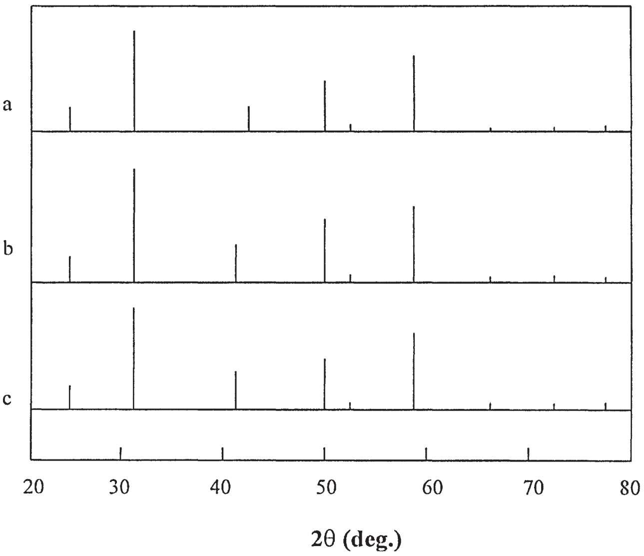

Figure 4. The XRD patterns of fresh $SrFeO_{3-0.190}$ (a) and $SrFeO_{3-0.382}Cl_{0.443}$ before (b) and after (c) 40 h of on-stream ODE reaction.

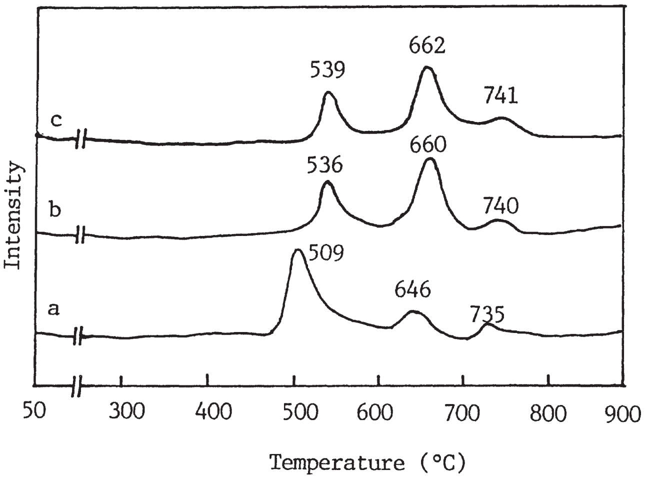

Figure 5. O_2-TPD profiles of fresh $SrFeO_{3-0.190}$ (a) and $SrFeO_{3-0.382}Cl_{0.443}$ before (b) and after (c) 40 h of on-stream ODE reaction.

3.4. O_2-TPD studies

Figure 5 shows the O_2-TPD profiles of the fresh $SrFeO_{3-0.190}$ and $SrFeO_{3-0.382}Cl_{0.443}$ samples; the O_2-TPD profile of a used $SrFeO_{3-0.382}Cl_{0.443}$ sample is also shown. There were three desorption peaks in each profile. For the $SrFeO_{3-0.190}$ sample (figure 5(a)), the peak at 509 °C was the largest, the two at 646 and 735 °C were relatively smaller. As for the $SrFeO_{3-0.382}Cl_{0.443}$ sample (figure 5(b)), compared to those of $SrFeO_{3-0.190}$, the intensity of the first peak at ca. 536 °C was smaller, whereas the second peak at ca. 660 °C was larger, and the third peak at 740 °C was wider. The O_2-TPD profiles of the fresh and used $SrFeO_{3-0.382}Cl_{0.443}$ samples were basically the same, indicating that the $SrFeO_{3-0.382}Cl_{0.443}$ catalyst had undergone no significant change in physico-chemical properties during the 40 h of ODE reaction.

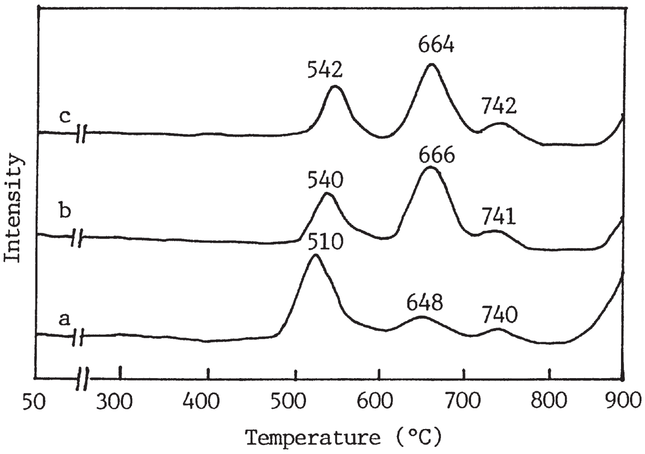

Figure 6. TPR profiles of fresh $SrFeO_{3-0.190}$ (a) and $SrFeO_{3-0.382}Cl_{0.443}$ before (b) and after (c) 40 h of on-stream ODE reaction.

3.5. TPR studies

Figure 6 shows the TPR profiles of $SrFeO_{3-0.190}$ and $SrFeO_{3-0.382}Cl_{0.443}$. There were three reduction bands with positions and relative strengths reflecting the O_2 desorption peaks of the O_2-TPD profiles in figure 5. For the $SrFeO_{3-0.190}$ catalyst (figure 6(a)), large reduction occurred at 510 °C, and there were two broad bands with smaller intensities at 648 and 740 °C. For the samples of fresh and used $SrFeO_{3-0.382}Cl_{0.443}$ (figure 6 (b) and (c)), the bands at ca. 666 °C were bigger in intensity than the first ones at ca. 542 °C. The third bands at ca. 740 °C were rather similar in the three profiles.

4. Discussion

It is well known that perovskite-type mixed oxide materials are good catalysts for the complete oxidation of hydrocarbons, carbon monoxide, and ammonia [24–26]. Over these catalysts, oxygen could be adsorbed easily to form surface oxygen species such as O_2^-, O_2^{2-}, and O^-. Most researchers believe that O^- is the active species for the total oxidation of hydrocarbons and carbon monoxide, and O^{2-} in the lattice is responsible for the selective oxidation of these substances [24,25,30]. However, in the oxidative dehydrogenation of ethane to ethene, dioxygen species such as $O_2^{\delta-}$ $(0 < \delta < 1)$, O_2^-, O_2^{n-} $(1 < n < 2)$, O_2^{2-} and monoxygen species such as O^- are thought to participate in the selective oxidation of ethane to ethene [15–23]. It is obvious that the kinds of oxygen adspecies and their distribution over the catalyst surfaces have direct influence on the catalytic performance. The increase of oxygen vacancies in the perovskite materials is beneficial for the adsorption of gaseous oxygen molecules to form oxygen adspecies active for complete oxidation reactions. On the other hand, the redox ability of B-site ions is determined by the oxidation states of the B-site ions and their relative content can also influence the catalytic performance of perovskites (ABO_3). The rise in Fe^{4+}/Fe ratio in $La_{1-x}Sr_xFeO_3$ (x = 0–1) is favourable to the generation of oxygen adspecies [26]. If one could modify the perovskite materials to give a suitable concentration of oxygen vacancies and ratio of various valencies of B-site cations, at which the selective oxidation reaction would be dominant, one would expect higher ethene selectivity.

By comparing the data in figure 1 (a) and (b), on the basis of similar specific surface area, one can conclude that the $SrFeO_{3-0.382}Cl_{0.443}$ catalyst was much superior to $SrFeO_{3-0.190}$ in ethane conversion and ethene selectivity. Under the reaction conditions of temperature $=$ 650 °C, C_2H_6/O_2 molar ratio $= 1/1$, space velocity $=$ 7000 $ml\,h^{-1}\,g^{-1}$, a $SrFeO_{3-0.190}$ catalyst showed 82.4% ethane conversion and 40.6% ethene selectivity (ethene yield $=$ 33.5%). A $SrFeO_{3-\delta}$ catalyst reported by Yi et al. [14] showed slightly better performance (C_2H_6 conversion $=$ 87%, C_2H_4 selectivity $=$ 43%, and C_2H_4 yield $=$ 37%) under similar conditions. The discrepancy could be due to deviation in the amounts of oxygen vacancies possessed by the two samples. Compared to $SrFeO_{3-\delta}$ or $SrFeO_{3-0.190}$, the Cl-doped $SrFeO_{3-0.382}Cl_{0.443}$ catalyst is much superior in catalytic performance: ethane conversion and ethene selectivity were 86.1 and 63.2%, respectively, giving a respectable ethene yield of 54.4%.

One should take note that the complete oxidation of C_2H_6 gives off much more heat than the ODE reaction. Over the $SrFeO_{3-0.382}Cl_{0.443}$ catalyst, with the increase of space velocity, C_2H_6 conversion and CO_x selectivity decreased whereas C_2H_4 selectivity increased (figure 2). It implied that the occurrence of hot spots on the catalyst surface was not significant. In other words, the excellent performance is a result of real catalysis of the Cl-doped perovskite material.

The oxidation of ethane involves several reactions:

$$C_2H_6 + (1/2)O_2 \rightarrow C_2H_4 + H_2O \tag{1}$$

$$C_2H_6 + (5/2)O_2 \rightarrow CO + 3H_2O \tag{2}$$

$$C_2H_6 + (7/2)O_2 \rightarrow 2CO_2 + 3H_2O \tag{3}$$

$$C_2H_6 + O_2 \rightarrow CO + CH_4 + H_2O \tag{4}$$

Compared to reactions (2), (3), and (4), reaction (1) consumes less amount of oxygen. At an oxygen conversion of 100%, ethane conversion and ethene selectivity could increase simultaneously if reactions (2), (3), and (4) were suppressed. In $SrFeO_{3-0.190}$, the nonstoichiometric amount of oxygen is 0.190. In $SrFeO_{3-0.382}Cl_{0.443}$, the Cl^- anions could enter positions previously occupied by O^{2-} ions and/or oxygen vacancies. If a O^{2-} ion is substituted by a Cl^- ion, in order to maintain electrical neutrality, one Cl^- ion has to enter an adjacent oxygen vacancy or the oxidation state of an iron cation has to decrease. As shown in table 1, the introduction of Cl^- ions into $SrFeO_{3-\delta}$ led to the increase rather than the decrease of Fe^{4+}/Fe ratio. This indicates that the Cl^- ions have occupied a certain amount of oxygen vacancies. Therefore, we suggest that the inclusion of chloride ions in the $SrFeO_{3-\delta}$ lattice has caused the bulk density of oxygen vacancies to decrease and the complete oxidation reactions were suppressed as a result.

The partial substitution of chloride ions for oxide ions did not induce any obvious change in crystal structure, i.e., the $SrFeO_{3-0.382}Cl_{0.443}$ sample retained an oxygen-deficient perovskite structure (figure 4). The Cl^- ions (radius 1.81 Å [31]) are fixed in the positions that are originally occupied by O^{2-} ions (radius 1.40 Å [31]). Based on the radii of Sr^{2+}, Fe^{3+}, Fe^{4+}, O^{2-}, and Cl^- ions [32,33], the tolerance factor [32], t, is in the range of 0.88–0.94, which is suitable for the formation of perovskite structure. Being larger in size, the Cl^- ions can enter into the $SrFeO_{3-\delta}$ lattice only in small quantities. The existence of a single phase of perovskite $SrFeO_{3-0.382}Cl_{0.443}$ means that this material is thermally stable and as a matter of fact, the leaching of Cl is not significant at the temperatures adopted for the ODE reaction. The result of chemical analysis also confirmed this point. In addition, compared to that of a fresh sample, no change was observed in the XRD pattern (figure 4(c)) of the $SrFeO_{3-0.382}Cl_{0.443}$ catalyst after 40 h of on-stream ODE reaction. It can be seen from figure 3 that the Cl-doped perovskite showed a sustainable activity within a period of 40 h. The stable catalytic performance of the perovskite-type chloro-oxide at 680 °C suggested that this material was an excellent and durable catalyst for the ODE reaction.

Generally speaking, the O_2-TPD profiles of most perovskites can be characterized by the appearance of the α and β desorption peaks. The α peak is due to the oxygen that is accommodated in the oxygen vacancies, while the β desorption is ascribable to the reduction of B-site cations [24]. The inclusion of Cl^- ions in $SrFeO_{3-\delta}$ gives rise to two effects: (i) the decrease in oxygen vacancies, i.e., the decrease of α oxygen; (ii) the rise in Fe^{4+}/Fe ratio, i.e., the increase of β oxygen desorption. As shown in figure 5, with the addition of Cl^- ions to $SrFeO_{3-0.190}$, the intensity of the first (α) peak decreased, whereas the second (β) peak increased in intensity, while the third (γ) peak widened. It is clear that the concentration and distribution of oxygen adspecies on $SrFeO_{3-0.382}Cl_{0.443}$ were different from those on $SrFeO_{3-\delta}$. At the moment, we are not sure of the role and nature of the γ oxygen. According to the activity data (figure 1), the $SrFeO_{3-0.382}Cl_{0.443}$ catalyst showed high ethene selectivity at the temperatures ranging from 480 to 560 °C and from 620 to 660 °C, coinciding the temperatures at which the α and β O_2 desorption peaks occurred (figure 5(b)). We suggest that the oxygen adspecies that desorbed at ca. 540 and ca. 660 °C are the active oxygen species for selective ethane oxidation. The TPR profile (figure 6(b)) of the $SrFeO_{3-0.382}Cl_{0.443}$ catalyst also demonstrated that there were more oxygen species available for the ODE reaction at ca. 666 °C.

5. Conclusion

The perovskite-type chloro-oxide catalyst has been shown to be a durable material for the selective oxidation of ethane. XRD results showed that both $SrFeO_{3-0.190}$ and $SrFeO_{3-0.382}Cl_{0.443}$ catalysts exhibited the structure of oxygen-deficient perovskite. The latter performed much better than the former in the ODE reaction. Over the $SrFeO_{3-0.382}Cl_{0.443}$ catalyst, under the conditions of reactant molar ratio $C_2H_6:O_2:N_2 = 2:1:3.7$, temperature $= 680\,^{\circ}C$, space velocity $= 6000$ ml h^{-1} g^{-1}, and pressure $=$ 1 atm, an ethane conversion of ca. 90% and an ethene selectivity of ca. 70% with an ethene yield of ca. 63% could be obtained. The O_2-TPD and TPR investigations illustrated that the introduction of chloride ions into the $SrFeO_{3-\delta}$ lattice would lead to the regulation of oxygen vacancies and Fe^{4+}/Fe ratio and, hence, the suppression of ethane and ethene deep oxidation. We envisage that perovskite-type halo-oxides of this kind are promising catalytic materials for the selective oxidation of light hydrocarbons.

Acknowledgement

The work described above was fully supported by a grant from the Research Grants Council of the Hong Kong Special Administration Region, China (Project No. HKBU 2050/97P). HXD thanks the HKBU for a Ph.D. Studentship.

References

[1] D. Wang, M.P. Rosynek and J.H. Lunsford, J. Catal. 151 (1995) 155.
[2] S.J. Conway and J.H. Lunsford, J. Catal. 131 (1991) 513.
[3] E.M. Kennedy and N.W. Cant, Appl. Catal. 87 (1992) 171.
[4] C.T. Au, X.P. Zhou and H.L. Wan, Catal. Lett. 40 (1996) 101.
[5] A. Erdöhelyi, F. Máté and F. Solymosi, J. Catal. 135 (1992) 563.
[6] A. Erdöhelyi and F. Solymosi, J. Catal. 129 (1991) 497.
[7] Y.F. Chang, G.A. Somorjai and H. Heinemann, J. Catal. 154 (1995) 24.
[8] T. Hayakawa, H. Orita, M. Shimizu, K. Takehira, A.G. Andersen, K. Nomura and Y. Ujihira, Catal. Lett. 16 (1992) 359.
[9] K. Omata, O. Yamazaki, K. Tomita and K. Fujimoto, J. Chem. Soc. Chem. Commun. (1994) 1647.
[10] Y.S. Lin and Y. Zeng, J. Catal. 164 (1996) 220.
[11] T. Nozaki and K. Fujimoto, AIChE J. 40 (1994) 870.
[12] J.E. ten Helshof, H.J.M. Bouwmeester and H. Verweeij, Appl. Catal. A 130 (1995) 195.
[13] T. Hayakawa, A.G. Andersen, H. Orita, M. Shimizu and K. Takehira, Catal. Lett. 16 (1992) 373.
[14] G.H. Yi, T. Hayakawa, A.G. Andersen, K. Suzuki, S. Hamakawa, A.P.E. York, M. Shimizu and K. Takehira, Catal. Lett. 38 (1996) 189.
[15] C.T. Au, H. He, S.Y. Lai and C.F. Ng, J. Catal. 159 (1996) 280.
[16] C.T. Au, Y.Q. Zhang, H. He, S.Y. Lai and C.F. Ng, J. Catal. 167 (1997) 354.
[17] C.T. Au, H. He, S.Y. Lai and C.F. Ng, Appl. Catal. 159 (1997) 133.
[18] C.T. Au, H. He, S.Y. Lai and C.F. Ng, J. Catal. 163 (1996) 399.
[19] C.T. Au, Y.W. Liu and C.F. Ng, J. Catal. 171 (1997) 231.
[20] C.T. Au, X.P. Zhou, Y.W. Liu, W.J. Ji and C.F. Ng, J. Catal. 174 (1998) 153.
[21] C.T. Au, K.D. Chen and C.F. Ng, Appl. Catal., in press.
[22] C.T. Au, K.D. Chen, H.X. Dai, Y.W. Liu and C.F. Ng, Appl. Catal., in press.
[23] C.T. Au, K.D. Chen, H.X. Dai, Y.W. Liu, J.Z. Luo and C.F. Ng, J. Catal. 179 (1998) 300.
[24] T. Seiyama, in: *Properties and Applications of Perovskite-Type Oxides*, eds. L.G. Tejuca and J.L.G. Fierro (1993) p. 215.
[25] B. Viswanathan, in: *Properties and Applications of Perovskite-Type Oxides*, eds. L.G. Tejuca and J.L.G. Fierro (1993) p. 271.
[26] Y. Wu, T. Yu, B.S. Dou, C.X. Wang, X.F. Xie, Z.L. Yu, S.R. Fan, Z.R. Fan and L.C. Wang, J. Catal. 120 (1989) 88.
[27] M.L. Rojas, J.L.G. Fierro, L.G. Tejuca and A.T. Bell, J. Catal. 124 (1990) 41.
[28] J. Mizusaki, M. Okayasu, S. Yamauchi and K. Fueki, J. Solid State Chem. 99 (1992) 166.
[29] N. Yamazoe, Y. Teraoka and T. Seiyama, Chem. Lett. (1981) 1767.
[30] J. Haber, in: *Surface Properties and Catalysis by Non-Metals*, eds. J.P. Bonnelle, B. Ihme and E. Derouane (Reidel, Dordrecht, 1983).
[31] F.A. Cotton and G. Wilkinson, *Advanced Inorganic Chemistry*, 3rd Ed. (Interscience, New York, 1972).
[32] J. Twu and P.K. Gallagher, in: *Properties and Applications of Perovskite-Type Oxides*, eds. L.G. Tejuca and J.L.G. Fierro (1993) p. 1.
[33] F.S. Galasso, *Perovskites and High Tc Superconductors* (OPA, Amsterdam, 1990) p. 51.